Effect of a biological parameter on the operating diagrams of a three-tiered model of anaerobic digestion

Sarra Nouaoura, Radhouane Fekih-Salem, Tewfik Sari

Effect of a biological parameter on the operating diagrams of a three-tiered model of anaerobic digestion

Sarra Nouaoura[1], **Radhouane Fekih-Salem**[*2,4], **Tewfik Sari**[3]

[1]Mathematics Department, University 20 august 1955, 21000, Skikda, Algeria
[2]University of Tunis El Manar, National Engineering School of Tunis, LAMSIN, 1002, Tunis, Tunisia
[3]ITAP, Univ Montpellier, INRAE, Institut Agro, Montpellier, France
[4]University of Monastir, Higher Institute of Computer Science of Mahdia, 5111, Mahdia, Tunisia

*E-mail : radhouene.fekihsalem@isima.rnu.tn

Abstract

The objective of this work is to perform the sensitivity study of the anaerobic mineralization of chlorophenol in a three-tiered food web model, with respect to the biological parameter. Recently, this study has been performed only numerically in the case with maintenance, and where only the chlorophenol input concentration is added to the system. Here, we construct analytically the operating diagrams, which depict the asymptotic behavior of the system according to operating parameters, in the particular case, then in the general case including the three input substrate concentrations, as well as maintenance. They show the effect of the biological parameter on the asymptotic behavior of the process by increasing this biological parameter.

Keywords

Anaerobic mineralization; Biological parameter; Operating diagram; Three-tiered food web; Chemostat.

I INTRODUCTION

The chemostat plays an important role as a model in various scientific fields such as mathematical biology. It is used as a model of the wastewater treatment process. It was performed to have a better understanding of anaerobic digestion (AD), which is an important process used in the treatment of wastewater and waste, including a large number of species that coexist in a very complex relationship. The full anaerobic digestion model (ADM1) developed in [1] contains 32 state variables and a large number of parameters.

The so-called AM2 model developed in [2] represents a two-tiered food web and provides a satisfactory prediction of the AD process by using the parameter identification theory and experimental data. In [10], the authors consider a three-tiered food web with three microbial species (chlorophenol and phenol degraders and hydrogenotrophic methanogen) that encapsulates the essence of the AD process. The corresponding model represents an extension of the model considered by [11].

Here, we reconsider the three-tiered model, developed in [10], which can be written as follows:

$$\begin{cases} \dot{X}_{\rm ch} &= (Y_{\rm ch} f_0\left(S_{\rm ch}, S_{\rm H_2}\right) - D - k_{\rm dec,ch}) X_{\rm ch} \\ \dot{X}_{\rm ph} &= (Y_{\rm ph} f_1\left(S_{\rm ph}, S_{\rm H_2}\right) - D - k_{\rm dec,ph}) X_{\rm ph} \\ \dot{X}_{\rm H_2} &= (Y_{\rm H_2} f_2\left(S_{\rm H_2}\right) - D - k_{\rm dec,H_2}) X_{\rm H_2} \\ \dot{S}_{\rm ch} &= D\left(S_{\rm ch}^{\rm in} - S_{\rm ch}\right) - f_0\left(S_{\rm ch}, S_{\rm H_2}\right) X_{\rm ch} \\ \dot{S}_{\rm ph} &= D\left(S_{\rm ph}^{\rm in} - S_{\rm ph}\right) + \frac{224}{208}\left(1 - Y_{\rm ch}\right) f_0\left(S_{\rm ch}, S_{\rm H_2}\right) X_{\rm ch} - f_1\left(S_{\rm ph}, S_{\rm H_2}\right) X_{\rm ph} \\ \dot{S}_{\rm H_2} &= D\left(S_{\rm H_2}^{\rm in} - S_{\rm H_2}\right) - \frac{16}{208} f_0\left(S_{\rm ch}, S_{\rm H_2}\right) X_{\rm ch} - f_2(S_{\rm H_2}) X_{\rm H_2} \\ &\quad + \frac{32}{224}(1 - Y_{\rm ph}) f_1\left(S_{\rm ph}, S_{\rm H_2}\right) X_{\rm ph}, \end{cases} \tag{1}$$

where $S_{\rm ch}$, $S_{\rm ph}$ and $S_{\rm H_2}$ are the chlorophenol, phenol and hydrogen substrate concentrations, respectively; $X_{\rm ch}$, $X_{\rm ph}$ and $X_{\rm H_2}$ are the chlorophenol, phenol and hydrogen degrader concentrations; D is the dilution rate; f_i, $i = 0, 1, 2$ are the specific growth rates; $S_{\rm ch}^{\rm in}$, $S_{\rm ph}^{\rm in}$ and $S_{\rm H_2}^{\rm in}$ are the inflowing concentrations in the chemostat; $k_{\rm dec,ch}$, $k_{\rm dec,ph}$ and $k_{\rm dec,H_2}$ are the maintenance (or decay) rates; $Y_{\rm ch}$, $Y_{\rm ph}$ and $Y_{\rm H_2}$ are the yield coefficients. The value $224/208\,(1 - Y_{\rm ch})$ is the fraction of chlorophenol converted to phenol, $32/224\,(1 - Y_{\rm ph})$ is the fraction of phenol that is transformed to hydrogen and $16/208$ is the fraction of hydrogen consumed by the chlorophenol degrader $X_{\rm ch}$. The growth functions take the following form:

$$f_0\left(S_{\rm ch}, S_{\rm H_2}\right) = \frac{k_{m,\rm ch} S_{\rm ch}}{K_{S,ch} + S_{\rm ch}} \frac{S_{H_2}}{K_{S,\rm H_2,c} + S_{\rm H_2}}, \quad f_1\left(S_{\rm ph}, S_{\rm H_2}\right) = \frac{k_{m,\rm ph} S_{\rm ph}}{K_{S,\rm ph} + S_{\rm ph}} \frac{1}{1 + S_{\rm H_2}/K_{I,\rm H_2}}, \tag{2}$$
$$f_2\left(S_{\rm H_2}\right) = \frac{k_{m,\rm H_2} S_{\rm H_2}}{K_{S,\rm H_2} + S_{\rm H_2}}.$$

Several authors have studied this three-tiered model (1), see recent works [3, 5, 6, 7, 8, 9, 10]. In [10] most of the results on the steady states of model (1) were obtained only numerically, using specific growth rates given in (1). They have numerically performed several operating diagrams with respect to the four operating parameters. Recently, a rigorous mathematical analysis of this model (1) was done in [8] with a general class of growth rates but only the chlorophenol is in the input. When maintenance is included, a numerical evidence shows that the positive steady state can destabilize through a supercritical Hopf bifurcation with the appearance of a stable periodic orbit [8] which was not depicted in [10]. The operating diagrams presented in [8] were obtained analytically in the case without maintenance and numerically in the case with maintenance. In [9], the authors have considered the three-tiered model in the case without maintenance.

In [5, 6], we have described analytically the necessary and sufficient existence and stability conditions of the steady states. The one parameter bifurcation diagrams of the three-tiered model presented in these works were analytically constructed in the cases with and without maintenance. They show that the model has in both cases rich dynamics including bistability, coexistence and occurrence of the limit cycle due to supercritical Hopf bifurcation. Recently in [7], the operating diagrams were performed theoretically by using the analytical results of the existence and stability conditions in [5, 6]. We highlighted the impact of the operating parameters on the asymptotic behavior of the model. We have compared our results with the findings of the numerical study in [10] where several regions have been omitted.

The operating diagrams show how behaves the system when the operating parameters are varying, such that the values of the biological parameters are fixed. This bifurcation diagram is very useful to understand the model from both the mathematical and biological points of view, and is often constructed both in the biological literature [10] and the mathematical literature [4, 8].

Our main aim in this work is to describe theoretically the operating diagram which determines the behavior of the system, in the particular case when only chlorophenol is in the input, then,

in the general case where the three substrates are in the input, with respect to the parameters D, $S_{\rm ch}^{\rm in}$, $S_{\rm ph}^{\rm in}$ and $S_{\rm H_2}^{\rm in}$. With this approach, we highlight how this diagram is affected by biological parameter variations, under the joined effect of the decay terms. This question was not considered in [10].

The paper is organized as follows. In section II, we present the steady states of the three-tiered model. Next, in section III, we describe analytically the operating diagrams in the case with maintenance terms. Finally, we discuss our results and some conclusions are drawn in section IV. In Appendix A, we present the change of variables that are used to simplify the analysis of the general model and we describe the results of [5, 6] on the existence and local stability of the steady states. The equations of the curves that delimit the regions of the operating diagrams are provided in Appendix B.

II STEADY STATES OF THE MODEL

The mathematical analysis of (1) given in [5, 6, 8] is carried out with a general class of growth functions, of which functions (2) are a particular example. Under these assumptions, system (1) can have up to eight possible steady states, labeled below as:

- SS1: the washout steady state where all populations are extinct.
- SS2: only the hydrogenotrophic methanogens are maintained ($X_{\rm H_2} > 0$).
- SS3: only the chlorophenol degraders are maintained ($X_{\rm ch} > 0$).
- SS4: only the hydrogenotrophic methanogens are washed out ($X_{\rm ch}$ and $X_{\rm ph} > 0$).
- SS5: only the phenol degraders are washed out ($X_{\rm ch}$ and $X_{\rm H_2} > 0$).
- SS6: all three populations are present ($X_{\rm ch}$, $X_{\rm ph}$ and $X_{\rm H_2} > 0$).
- SS7: only the phenol degraders are present ($X_{\rm ph} > 0$).
- SS8: only the chlorophenol degraders are washed out ($X_{\rm ph}$ and $X_{\rm H_2} > 0$).

From [6], the components of these steady states are given in Table 2. The conditions of their existence and stability are provided in Table 3.

Remark 1:
The steady state SS1 always exists. There exist at most two steady states of the form SS4, that we denote by SS4^1 and SS4^2. The other steady states are unique if they exist (see [8]).

III OPERATING DIAGRAM

Our objective now is to describe analytically the operating diagram of system (1). The biological parameter values used for plotting the operating diagrams are provided in Table 1 of [10]. The boundaries of the regions in the operating diagram are surfaces, where bifurcations occur. Using Table 3, these boundaries are the surfaces Γ_i, $i = 1, \ldots, 12$ of the $\left(D, S_{\rm ch}^{\rm in}, S_{\rm ph}^{\rm in}, S_{\rm H_2}^{\rm in}\right)$-space and defined in Table 4. Using our result in [7], we recall the existence and the stability of the steady states of (1) according to the twenty-seven regions J_i, $i = 1, \ldots, 27$ of the operating diagrams determined in Table 1.

Remark 2:
Each region is denoted by its steady states, indicating which are stable and which are unstable. For instance, the region $J_6 = (2, 1)$ in Table 1 means that when the operating parameters are taken in J_6, then the steady state SS2 is stable, the steady state SS1 is unstable, and there is no other steady state.

Table 1: Existence and stability of steady states in the regions of the operating diagrams of Figs. 1 to 8.

Region	*SS1*	*SS2*	*SS3*	*SS4*^{1}	*SS4*^{2}	*SS5*	*SS6*	*SS7*	*SS8*	*Color*
$\mathcal{J}_1 = (1)$	*S*									*Red*
$\mathcal{J}_2 = (14^2, 4^1)$	*S*			*U*	*S*					*green*
$\mathcal{J}_3 = (16, 4^1 4^2)$	*S*			*U*	*U*		*S*			*Yellow*
$\mathcal{J}_4 = (1, 4^1 4^2)$	*S*			*U*	*U*					*Blue*
$\mathcal{J}_5 = (1, 4^1 4^2 6)$	*S*			*U*	*U*		*U*			*Blueviolet*
$\mathcal{J}_6 = (2, 1)$	*U*	*S*								*White*
$\mathcal{J}_7 = (2, 13)$	*U*	*S*	*U*							*White*
$\mathcal{J}_8 = (5, 123)$	*U*	*U*	*U*			*S*				*Pink*
$\mathcal{J}_9 = (3, 12)$	*U*	*U*	*S*							*DimGray*
$\mathcal{J}_{10} = (34^2, 124^1)$	*U*	*U*	*S*	*U*	*S*					*Olive*
$\mathcal{J}_{11} = (6, 1234^2)$	*U*	*U*	*U*		*U*		*S*			*Magenta*
$\mathcal{J}_{12} = (6, 1234^2 5)$	*U*	*U*	*U*		*U*	*U*	*S*			*Magenta*
$\mathcal{J}_{13} = (4^2, 123)$	*U*	*U*	*U*		*S*					*Purple*
$\mathcal{J}_{14} = (6, 1234^2 8)$	*U*	*U*	*U*		*U*		*S*		*U*	*Magenta*
$\mathcal{J}_{15} = (6, 1234^2 58)$	*U*	*U*	*U*		*U*	*U*	*S*		*U*	*Magenta*
$\mathcal{J}_{16} = (6, 12358)$	*U*	*U*	*U*			*U*	*S*		*U*	*Magenta*
$\mathcal{J}_{17} = (8, 123)$	*U*	*U*	*U*						*S*	*Orange*
$\mathcal{J}_{18} = (8, 12)$	*U*	*U*							*S*	*Orange*
$\mathcal{J}_{19} = (6, 1235)$	*U*	*U*	*U*			*U*	*S*			*Magenta*
$\mathcal{J}_{20} = (8, 1234^2)$	*U*	*U*	*U*		*U*				*S*	*Orange*
$\mathcal{J}_{21} = (8, 1234^1 4^2)$	*U*	*U*	*U*	*U*	*U*				*S*	*Orange*
$\mathcal{J}_{22} = (., 12)$	*U*	*U*								*Turquoise*
$\mathcal{J}_{23} = (., 123)$	*U*	*U*	*U*							*Khaki*
$\mathcal{J}_{24} = (., 1238)$	*U*	*U*	*U*						*U*	*Green*
$\mathcal{J}_{25} = (., 1234^1 4^2 8)$	*U*	*U*	*U*	*U*	*U*				*U*	*Chocolate*
$\mathcal{J}_{26} = (., 1234^2 8)$	*U*	*U*	*U*		*U*				*U*	*Tan*
$\mathcal{J}_{27} = (., 128)$	*U*	*U*							*U*	*SlateGray*

The representation of the regions $\mathcal{J}_i$, $i = 1, \ldots, 27$ in the four-dimensional $\left(D, S^{\text{in}}_{\text{ch}}, S^{\text{in}}_{\text{ph}}, S^{\text{in}}_{\text{H}_2}\right)$-space is not legible enough. For this reason, we will fix the values for $S^{\text{in}}_{\text{ph}}$ and $S^{\text{in}}_{\text{H}_2}$ and show the regions of existence and stability in the $\left(S^{\text{in}}_{\text{ch}}, D\right)$-plane. The intersections of the surfaces Γ_i, $i = 1 \ldots, 10$ with the $\left(S^{\text{in}}_{\text{ch}}, D\right)$-plane are curves of functions of D. However, the intersections of surfaces Γ_{11} and Γ_{12} with the $\left(S^{\text{in}}_{\text{ch}}, D\right)$-plane are straight lines. The other cases with $S^{\text{in}}_{\text{ph}} = 0$ or $S^{\text{in}}_{\text{H}_2} = 0$ were analyzed by the same way (see [7, 10]).

Following [8, 10], we consider two cases to examine the effect of the operating parameters $S^{\text{in}}_{\text{ph}}$ and $S^{\text{in}}_{\text{H}_2}$ on the behavior of the model. First, only chlorophenol input is added to the system ($S^{\text{in}}_{\text{ph}} = S^{\text{in}}_{\text{H}_2} = 0$). Then, the hydrogen and phenol inputs are added to the system ($S^{\text{in}}_{\text{ph}} = 1$ and $S^{\text{in}}_{\text{H}_2} = 2.67 \times 10^{-2}$). In addition, we consider four cases to examine the effect of the biological parameter $\text{K}_{\text{S,H}_2,\text{c}}$, on the behavior of the model, as in [8]. The values of the biological parameter $\text{K}_{\text{S,H}_2,\text{c}}$ are given in Table 5.

3.1 Only chlorophenol is in the input

Assume that $S^{\text{in}}_{\text{ph}} = S^{\text{in}}_{\text{H}_2} = 0$, we plot in the following the operating diagrams corresponding to four cases which obtained with the numerical parameter values of $\text{K}_{\text{S,H}_2,\text{c}}$.

3.1.1 *Operating diagrams: case (1)*

First, we consider the case of Fig. 4 in [8] where $K_{\mathrm{S,H_2,c}} = 10^{-6}$. The operating diagram in the plane $\left(S_{\mathrm{ch}}^{\mathrm{in}}, D\right)$ is shown in Fig. 1 which highlights the existence of the region $\mathcal{J}_5$ of instability of SS6 which was already detected in [8], a fact that was not reported in [10]. Note that, each region that has a different asymptotic behavior is colored by a distinct color as in [8]. Therefore,

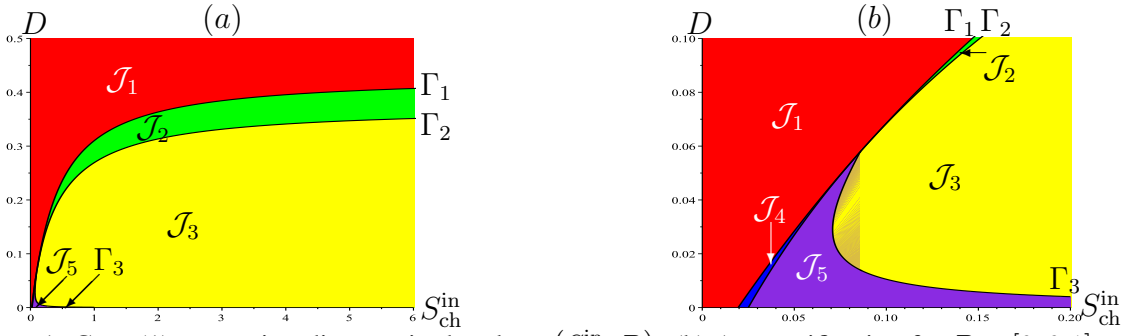

Figure 1: Case (1): operating diagram in the plane $\left(S_{\mathrm{ch}}^{\mathrm{in}}, D\right)$. (b) A magnification for $D \in [0, 0.1]$.

our theoretical study shows the same behavior as Figs. 8 and 9 in [8] and confirms the numerical findings presented in [8], in the case with maintenance.

3.1.2 *Operating diagrams: case (2)*

In the following, we study the operating diagrams of system (1) in the $\left(S_{\mathrm{ch}}^{\mathrm{in}}, D\right)$-plane by assuming a small increase to the biological parameter $K_{\mathrm{S,H_2,c}} = 4 \times 10^{-6}$ as in Fig. 5 of [8].

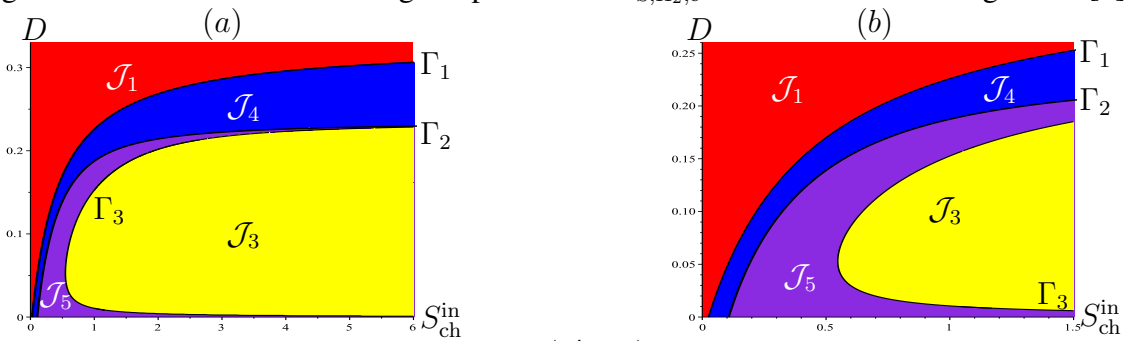

Figure 2: Case (2): operating diagram in the plane $\left(S_{\mathrm{ch}}^{\mathrm{in}}, D\right)$. (b) A magnification for $D \in [0, 0.26]$.

Increasing $K_{\mathrm{S,H_2,c}}$ leads to the disappearance of the bistability region $\mathcal{J}_2$ of the steady states SS1 and SS4[2] and to changes in the size of the existence and stability regions of the other steady states. Actually, the behavior of the system when $K_{\mathrm{S,H_2,c}} = 4 \times 10^{-6}$ was already clarified in [8], where the instability of SS3 has been studied numerically in the case with maintenance. Thus, our theoretical study confirms the numerical findings presented in [8].

3.1.3 *Operating diagrams: case (3)*

In the following, we analyze the effect of the biological parameter $K_{\mathrm{S,H_2,c}}$ on the behavior of the process. By comparing with the results obtained in the previous subsection, we increase the half-saturation constant $K_{\mathrm{S,H_2,c}}$ of the chlorophenol degrader on the hydrogen from 4×10^{-6} to 6×10^{-6}. The operating diagrams shown in Fig. 3 produce similar results as shown in the comparison of Fig. 2, with variations only in their shape and extent. However, Fig. 3 shows the

effect of the parameter $K_{\mathrm{S,H_2,c}}$ on the size of the regions, where the regions $\mathcal{J}_3$ and $\mathcal{J}_5$ diminish.

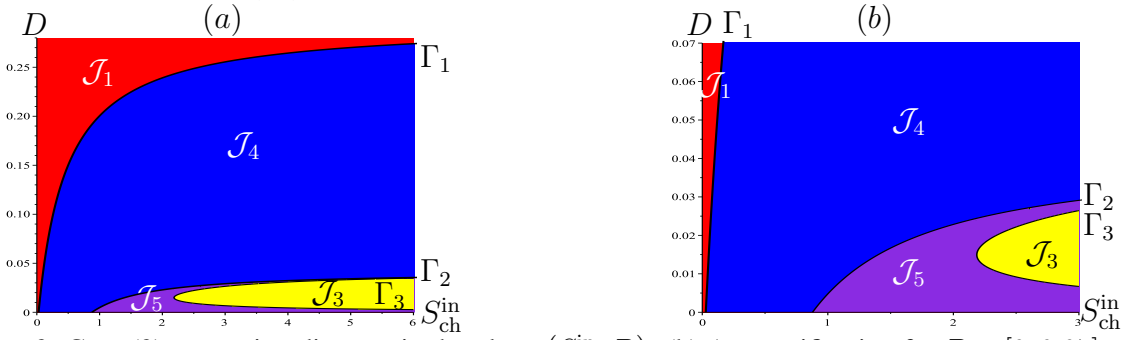

Figure 3: Case (3): operating diagram in the plane $\left(S^{\mathrm{in}}_{\mathrm{ch}}, D\right)$. (b) A magnification for $D \in [0, 0.07]$.

3.1.4 Operating diagrams: case (4)

Increasing once again the biological parameter $K_{\mathrm{S,H_2,c}}$, when we consider $K_{\mathrm{S,H_2,c}} = 7 \times 10^{-6}$ corresponding to case (c) in [8]. The operating diagram in the plane $\left(S^{\mathrm{in}}_{\mathrm{ch}}, D\right)$ is shown in Fig. 4. We have seen in the operating diagram presented in Fig. 4 that the steady states SS4[2] never stable and SS3 never exist, since I_2 (I_2 defined in Table 1 in [6]) is empty. Fig. 4 is the

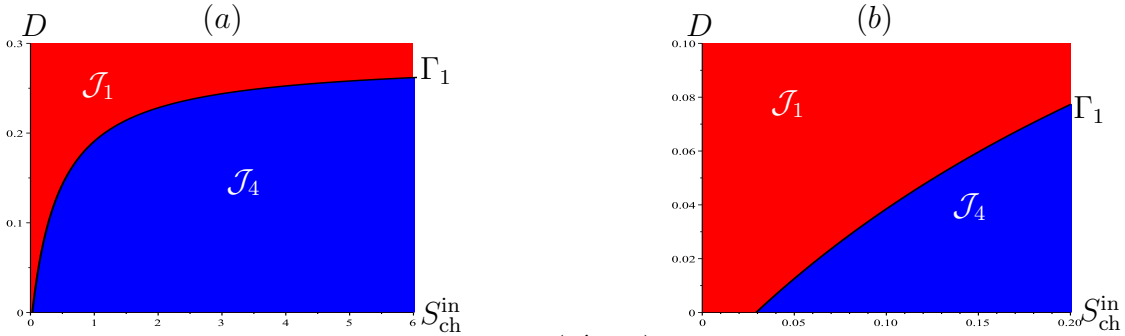

Figure 4: Case (4): operating diagram in the plane $\left(S^{\mathrm{in}}_{\mathrm{ch}}, D\right)$. (b) A magnification for $D \in [0, 0.1]$.

same as Fig. 12 in [8], which is obtained analytically. Thus, our theoretical study confirms the numerical results given in [8], such as Fig. 4 shows the same behavior as Fig. 12 in [8] achieved only numerically.

3.2 Hydrogen and phenol are added in the input

3.2.1 Operating diagrams: case (1)

We construct the operating diagram of system (1) in the $\left(S^{\mathrm{in}}_{\mathrm{ch}}, D\right)$-plane, assuming that $\mathrm{K_{S,H_2,c}} = 10^{-6}$ as in the case of Fig. 5(d) in [10]. Fig. 5 shows that the operating diagram in the $\left(S^{\mathrm{in}}_{\mathrm{ch}}, D\right)$-plane. The magnifications (b)–(c) put in evidence the regions $\mathcal{J}_i$, $i = 10, 11, 12, 15, 17, 18, 19$. Note that all asymptotic behaviors were detected in Fig. 5(d) of [10].

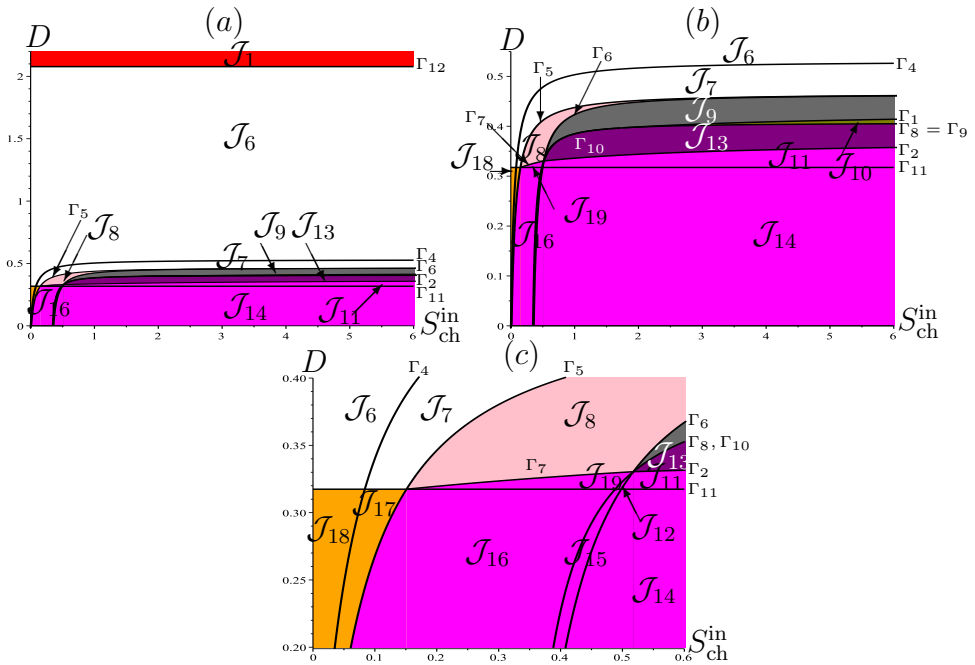

Figure 5: Case (1): operating diagram in the plane $\left(S^{in}_{ch}, D\right)$. Magnifications (b) for $D \in [0, 0.55]$, (c) for $D \in [0.2, 0.4]$.

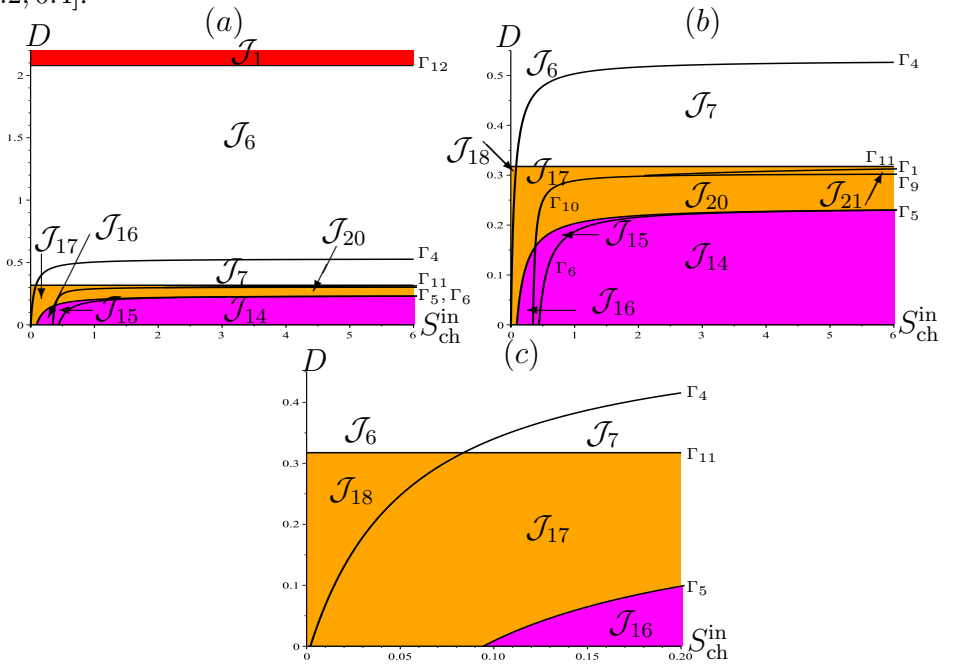

Figure 6: Case (2): operating diagram in the plane $\left(S^{in}_{ch}, D\right)$. Magnifications (b) for $D \in [0, 0.55]$, (c) for $D \in [0, 0.45]$.

3.2.2 Operating diagrams: case (2)

Considering the biological parameter $K_{S,H_2,c} = 4 \times 10^{-6}$ as in case (b) of [8], we represente the operating diagrams in the $\left(S^{in}_{ch}, D\right)$-plane in Fig. 6. The magnifications shown in Fig. 6(b)-(c) put in evidence the regions $\mathcal{J}_{18}$ and $\mathcal{J}_{18}$. Increasing $K_{S,H_2,c}$ leads to the disappearance of the bistability region $\mathcal{J}_{10}$ of the steady states SS3 and SS4[2], the stability regions $\mathcal{J}_8$, $\mathcal{J}_9$ and $\mathcal{J}_{13}$ of SS5, SS3 and SS4[2], respectively. Moreover, there is a change in the size of the existence and stability regions of the other steady states and the emergent of the stability region $\mathcal{J}_{21}$ of the steady state SS8, where only the chlorophenol degraders are eliminated.

3.2.3 *Operating diagrams: case (3)*

In the following, we increase $K_{\mathrm{S,H_2,c}}$ from 4×10^{-6} to 6×10^{-6} in order to compare with the results obtained in the previous subsection. To this end, we describe the operating diagrams in the plane $\left(S_{\mathrm{ch}}^{\mathrm{in}}, D\right)$. Fig. 7 show that the regions $\mathcal{J}_i$, $i = 1, 6, 7, 14, \ldots, 18, 20, 21$ are similar to those in the comparison of Fig. 6, with variations only in their shape and extent. Note that, the parameter $K_{\mathrm{S,H_2,c}}$ has a effect on the disappearance of the stability region $\mathcal{J}_{16}$ of SS6 and the size of the regions, where the regions $\mathcal{J}_{14}$ and $\mathcal{J}_{15}$ diminish.

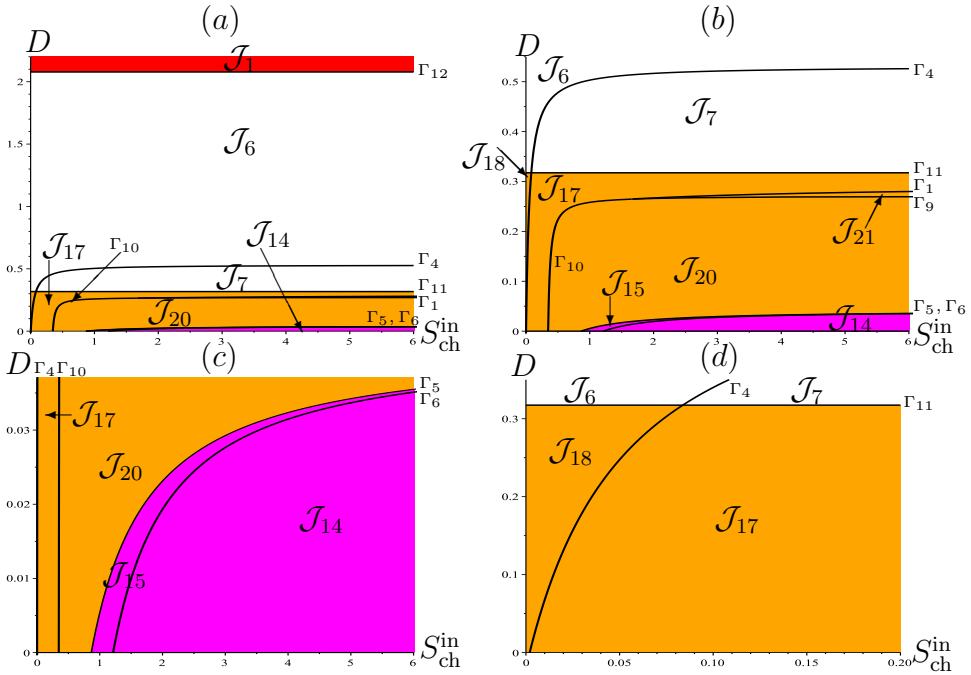

Figure 7: Case (3): operating diagram in the plane $\left(S_{\mathrm{ch}}^{\mathrm{in}}, D\right)$. Magnifications (b) for $D \in [0, 0.55]$, (c) for $D \in [0, 0.37]$, (d) for $D \in [0, 0.35]$.

3.2.4 *Operating diagrams: case (4)*

We increase once again the biological parameter $K_{\mathrm{S,H_2,c}} = 7 \times 10^{-6}$ as in case (c) of [8]. Fig. 8 illustrates the operating diagrams in the plane $\left(S_{\mathrm{ch}}^{\mathrm{in}}, D\right)$. From these diagrams, the new regions $\mathcal{J}_i$, $i = 22, \ldots, 27$ appear under the inffuence of the parameter $K_{\mathrm{S,H_2,c}}$. Note that the steady states SS2 and SS8 never stable and SS6 never exists, since I_2 is empty.

IV CONCLUSION

In this work, we have reconsidered the three-tiered microbial model (1) which was studied numerically in [8, 10]. Our aim was to perform analytically the operating diagrams, by plotting the curves that separate their various regions. Hence, the regions of the operating diagrams are constructed analytically by using the mathematical analysis obtained in our previous studies, and there is no requirement for time-consuming algorithms to generate the plots, as in the numerical method in [8, 10]. Moreover, by these operating diagrams, we illustrated its dependence on the biological parameter of the process. Our analytical study considers the effects of the three substrate inflowing concentrations, together with the effects of maintenance on the behavior of the model.

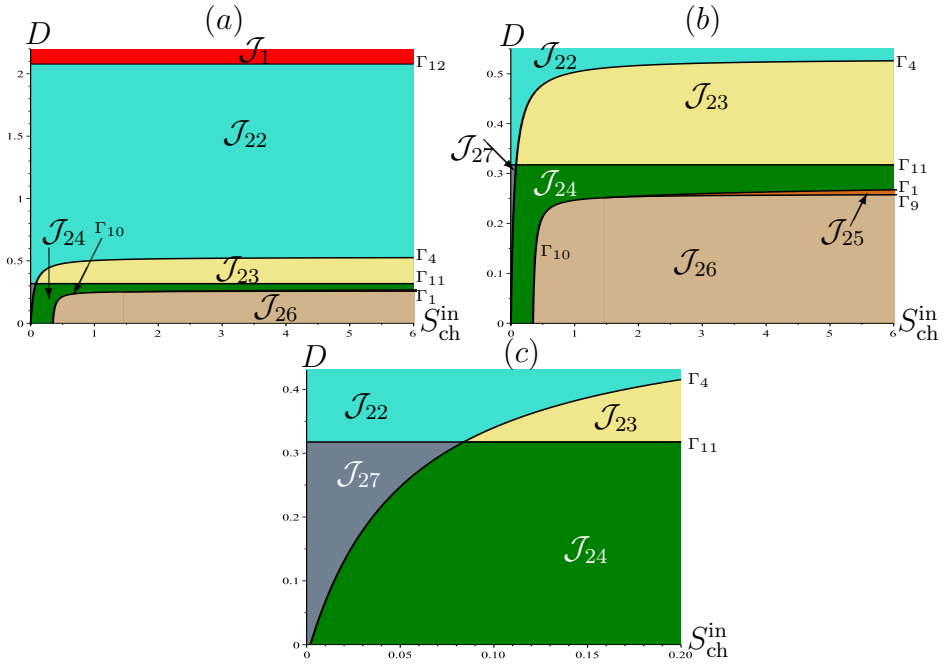

Figure 8: Case (4): operating diagram in the plane $\left(S_{\text{ch}}^{\text{in}}, D\right)$. Magnifications (b) for $D \in [0, 0.55]$, (c) for $D \in [0, 0.43]$.

Our theoretical description of the operating diagrams in the $\left(S_{\text{ch}}^{\text{in}}, D\right)$-plane provide the dynamical behavior of the process, according to the control parameters $S_{\text{ch}}^{\text{in}}$, $S_{\text{ph}}^{\text{in}}$, $S_{\text{H}_2}^{\text{in}}$ and D. For various values of the control parameters $K_{\text{S,H}_2\text{,c}}$, our operating diagrams in the plane $\left(S_{\text{ch}}^{\text{in}}, D\right)$ of Figs 1 to 8, in both cases where only chlorophenol is in the input and when the three input substrates are included, prove that the variation in the biological parameter $K_{\text{S,H}_2\text{,c}}$ can destabilize the steady state and it can also modify the shape of the regions. Moreover, it has also an effect on the appearance and the disappearance of some regions. This sensitivity study was not performed neither theoretically nor numerically in [8, 10].

A MODEL ANALYSIS

In this section, we recall from [5, 6] the main results of existence and stability of all steady states of system (1). Following [8], we can rescale model (1) to reduce the number of yield parameters and ease the mathematical analysis. We use the following change of variables:

$$x_0 = \frac{Y}{Y_0} X_{\text{ch}},\ x_1 = \frac{Y_4}{Y_1} X_{\text{ph}},\ x_2 = \frac{1}{Y_2} X_{\text{H}_2},\ s_0 = Y S_{\text{ch}},\ s_1 = Y_4 S_{\text{ph}},\ s_2 = S_{\text{H}_2}, \tag{3}$$

where the yield coefficients are

$$Y_0 = Y_{\text{ch}},\ Y_1 = Y_{\text{ph}},\ Y_2 = Y_{\text{H}_2},\ Y_3 = \tfrac{224}{208}(1 - Y_0),\ Y_4 = \tfrac{32}{224}(1 - Y_1),$$

with $Y = Y_3 Y_4$ and $\omega = \frac{16}{208Y}$. The inflowing concentrations are:

$$s_0^{\text{in}} = Y S_{\text{ch}}^{\text{in}}, \quad s_1^{\text{in}} = Y_4 S_{\text{ph}}^{\text{in}}, \quad s_2^{\text{in}} = S_{\text{H}_2}^{\text{in}}, \tag{4}$$

the death rates are $a_0 = k_{\text{dec,ch}}$, $a_1 = k_{\text{dec,ph}}$ and $a_2 = k_{\text{dec,H}_2}$. Under the scaling (3), the growth functions become:

$$\mu_0(s_0, s_2) = \frac{m_0 s_0}{K_0 + s_0} \frac{s_2}{L_0 + s_2},\ \mu_1(s_1, s_2) = \frac{m_1 s_1}{K_1 + s_1} \frac{1}{1 + s_2/K_I},\ \mu_2(s_2) = \frac{m_2 s_2}{K_2 + s_2}, \tag{5}$$

where

$$m_0 = Y_0 k_{m,\mathrm{ch}}, K_0 = Y K_{S,\mathrm{ch}}, L_0 = K_{S,\mathrm{H_2,c}}, m_1 = Y_1 k_{m,\mathrm{ph}},$$
$$K_1 = Y_4 K_{S,\mathrm{ph}}, K_I = K_{I,\mathrm{H_2}}, m_2 = Y_2 k_{m,\mathrm{H_2}}, K_2 = K_{S,\mathrm{H_2}}.$$

Using the change of variables (3) and (4), and Table 2 in [6], we can recall now the steady states of system (1) in Table 2. From Table 3 in [5] and the change of variables (4), all necessary and sufficient existence and stability conditions of the steady states of (1) in the case with maintenance are stated in Table 3.

Table 2: The steady states of (1). The function μ_i are given by (5). The function M_i, ψ_i and Ψ are given in Table 11 in [6]. For the general case, the functions are given in Table 1 in [6].

	s_0, s_1, s_2	x_0, x_1, x_2
SS1	$s_0 = Y S^{\mathrm{in}}_{\mathrm{ch}}$, $s_1 = Y_4 S^{\mathrm{in}}_{\mathrm{ph}}$, $s_2 = S^{\mathrm{in}}_{\mathrm{H_2}}$	$x_0 = 0, x_1 = 0, x_2 = 0$
SS2	$s_0 = Y S^{\mathrm{in}}_{\mathrm{ch}}$, $s_1 = Y_4 S^{\mathrm{in}}_{\mathrm{ph}}$, $s_2 = M_2(D + a_2)$	$x_0 = 0, x_1 = 0, x_2 = \frac{D}{D+a_2}\left(S^{\mathrm{in}}_{\mathrm{H_2}} - s_2\right)$
SS3	$s_0 = s_0\left(D, S^{\mathrm{in}}_{\mathrm{ch}}, S^{\mathrm{in}}_{\mathrm{H_2}}\right)$ is a solution of $\psi_0(s_0) = D + a_0$, $s_1 = Y_4 S^{\mathrm{in}}_{\mathrm{ph}} + Y S^{\mathrm{in}}_{\mathrm{ch}} - s_0$ $s_2 = S^{\mathrm{in}}_{\mathrm{H_2}} - \omega\left(Y S^{\mathrm{in}}_{\mathrm{ch}} - s_0\right)$	$x_0 = \frac{D}{D+a_0}\left(Y S^{\mathrm{in}}_{\mathrm{ch}} - s_0\right), x_1 = 0, x_2 = 0$
SS4	$s_2 = s_2\left(D, S^{\mathrm{in}}_{\mathrm{ch}}, S^{\mathrm{in}}_{\mathrm{ph}}, S^{\mathrm{in}}_{\mathrm{H_2}}\right)$ is a solution of $\Psi(s_2, D) = (1-\omega) Y S^{\mathrm{in}}_{\mathrm{ch}} + Y_4 S^{\mathrm{in}}_{\mathrm{ph}} + S^{\mathrm{in}}_{\mathrm{H_2}}$ $s_0 = M_0(D + a_0, s_2)$, $s_1 = M_1(D + a_1, s_2)$	$x_0 = \frac{D}{D+a_0}\left(Y S^{\mathrm{in}}_{\mathrm{ch}} - s_0\right)$, $x_1 = \frac{D}{D+a_1}\left(Y S^{\mathrm{in}}_{\mathrm{ch}} + Y_4 S^{\mathrm{in}}_{\mathrm{ph}} - s_0 - s_1\right)$, $x_2 = 0$
SS5	$s_0 = M_0(D + a_0, M_2(D + a_2))$, $s_1 = Y S^{\mathrm{in}}_{\mathrm{ch}} + Y_4 S^{\mathrm{in}}_{\mathrm{ph}} - s_0$, $s_2 = M_2(D + a_2)$	$x_0 = \frac{D}{D+a_0}\left(Y S^{\mathrm{in}}_{\mathrm{ch}} - s_0\right), x_1 = 0,$ $x_2 = \frac{D}{D+a_2}\left(S^{\mathrm{in}}_{\mathrm{H_2}} - s_2 - \omega\left(Y S^{\mathrm{in}}_{\mathrm{ch}} - s_0\right)\right)$
SS6	$s_0 = M_0(D + a_0, M_2(D + a_2))$, $s_1 = M_1(D + a_1, M_2(D + a_2))$, $s_2 = M_2(D + a_2)$	$x_0 = \frac{D}{D+a_0}\left(Y S^{\mathrm{in}}_{\mathrm{ch}} - s_0\right)$, $x_2 = \frac{D}{D+a_2}\left((1-\omega)\left(Y S^{\mathrm{in}}_{\mathrm{ch}} - s_0\right) + Y_4 S^{\mathrm{in}}_{\mathrm{ph}} + S^{\mathrm{in}}_{\mathrm{H_2}} - s_1 - s_2\right)$, $x_1 = \frac{D}{D+a_1}\left(Y S^{\mathrm{in}}_{\mathrm{ch}} + Y_4 S^{\mathrm{in}}_{\mathrm{ph}} - s_0 - s_1\right)$
SS7	$s_0 = Y S^{\mathrm{in}}_{\mathrm{ch}}$, $s_1 = s_1\left(D, S^{\mathrm{in}}_{\mathrm{ph}}, S^{\mathrm{in}}_{\mathrm{H_2}}\right)$ is a solution of $\psi_1(s_1) = D + a_1$, $s_2 = Y_4 S^{\mathrm{in}}_{\mathrm{ph}} + S^{\mathrm{in}}_{\mathrm{H_2}} - s_1$	$x_0 = 0, x_1 = \frac{D}{D+a_1}\left(Y_4 S^{\mathrm{in}}_{\mathrm{ph}} - s_1\right), x_2 = 0$
SS8	$s_0 = Y S^{\mathrm{in}}_{\mathrm{ch}}$, $s_1 = M_1(D + a_1, M_2(D + a_2))$, $s_2 = M_2(D + a_2)$	$x_0 = 0, x_1 = \frac{D}{D+a_1}\left(Y_4 S^{\mathrm{in}}_{\mathrm{ph}} - s_1\right)$, $x_2 = \frac{D}{D+a_2}\left(Y_4 S^{\mathrm{in}}_{\mathrm{ph}} + S^{\mathrm{in}}_{\mathrm{H_2}} - s_1 - s_2\right)$

Remark 3:
In the case without maintenance, the necessary and sufficient conditions of existence and local stability can be deduced from Table 3 by taking $a_i = 0$, except for the stability condition of SS6 which is given by

$$\phi_3(D) \geq 0 \qquad \text{or} \quad \phi_3(D) < 0, \quad \phi_4(D, S^{\mathrm{in}}_{\mathrm{ch}}, S^{\mathrm{in}}_{\mathrm{ph}}, S^{\mathrm{in}}_{\mathrm{H_2}}) > 0, \tag{6}$$

where the function ϕ_3 is defined in Table 1 in [6] and ϕ_4 is defined by:

$$\begin{aligned}\phi_4(D, S^{\mathrm{in}}_{\mathrm{ch}}, S^{\mathrm{in}}_{\mathrm{ph}}, S^{\mathrm{in}}_{\mathrm{H_2}}) = {} & (EIx_0x_2 + EG\phi_3(D)x_0x_1)(Ix_2 + (G+H)x_1 + (E+\omega F)x_0) \\ & + (Ix_2 + (G+H)x_1 + \omega F x_0) GI x_1 x_2,\end{aligned} \tag{7}$$

with

$$E = \frac{\partial \mu_0}{\partial s_0}(s_0, s_2),\ F = \frac{\partial \mu_0}{\partial s_2}(s_0, s_2),\ G = \frac{\partial \mu_1}{\partial s_1}(s_1, s_2),\ H = -\frac{\partial \mu_1}{\partial s_2}(s_1, s_2),\ I = \frac{d\mu_2}{ds_2}(s_2).$$

Table 3: Case of maintenance: necessary and sufficient existence and local stability conditions of steady states of (1). The functions c_3, c_5, r_3 and r_5, used in the stability condition of SS6, are given in Table 2 in [5]. All other functions are given in Table 8 of [5].

	Existence conditions	Stability conditions
SS1	always exists	$\mu_0\left(S_{\text{ch}}^{\text{in}}Y, S_{\text{H}_2}^{\text{in}}\right) < D + a_0$, $\mu_1\left(S_{\text{ph}}^{\text{in}}Y_4, S_{\text{H}_2}^{\text{in}}\right) < D + a_1$, $\mu_2\left(S_{\text{H}_2}^{\text{in}}\right) < D + a_2$
SS2	$\mu_2\left(S_{\text{H}_2}^{\text{in}}\right) > D + a_2$	$S_{\text{ch}}^{\text{in}}Y < \varphi_0(D)$, $S_{\text{ph}}^{\text{in}}Y_4 < \varphi_1(D)$
SS3	$\mu_0\left(S_{\text{ch}}^{\text{in}}Y, S_{\text{H}_2}^{\text{in}}\right) > D + a_0$	$\mu_1\left(S_{\text{ch}}^{\text{in}}Y + S_{\text{ph}}^{\text{in}}Y_4 - s_0, S_{\text{H}_2}^{\text{in}} - \omega\left(S_{\text{ch}}^{\text{in}}Y - s_0\right)\right) < D + a_1$ $S_{\text{H}_2}^{\text{in}} - \omega S_{\text{ch}}^{\text{in}}Y < M_2(D + a_2) - \omega\varphi_0(D)$ with s_0 solution of equation $\psi_0(s_0) = D + a_0$
SS4	$(1-\omega)S_{\text{ch}}^{\text{in}}Y + S_{\text{ph}}^{\text{in}}Y_4 + S_{\text{H}_2}^{\text{in}} \geq \phi_1(D)$, $S_{\text{ch}}^{\text{in}}Y > M_0\left(D + a_0, s_2\right)$, $S_{\text{ch}}^{\text{in}}Y + S_{\text{ph}}^{\text{in}}Y_4 > M_0\left(D + a_0, s_2\right) + M_1\left(D + a_1, s_2\right)$, with s_2 solution of equation $\Psi(s_2) = (1-\omega)S_{\text{ch}}^{\text{in}}Y + S_{\text{ph}}^{\text{in}}Y_4 + S_{\text{H}_2}^{\text{in}}$	$(1-\omega)S_{\text{ch}}^{\text{in}}Y + S_{\text{ph}}^{\text{in}}Y_4 + S_{\text{H}_2}^{\text{in}} < \phi_2(D)$, $\dfrac{\partial\Psi}{\partial s_2}(s_2, D) > 0$ and $\phi_3(D) > 0$
SS5	$S_{\text{ch}}^{\text{in}}Y > \varphi_0(D)$, $S_{\text{H}_2}^{\text{in}} - \omega S_{\text{ch}}^{\text{in}}Y > M_2(D + a_2) - \omega\varphi_0$	$S_{\text{ch}}^{\text{in}}Y + S_{\text{ph}}^{\text{in}}Y_4 < \varphi_0(D) + \varphi_1(D)$
SS6	$(1-\omega)S_{\text{ch}}^{\text{in}}Y + S_{\text{ph}}^{\text{in}}Y_4 + S_{\text{H}_2}^{\text{in}} > \phi_2(D)$, $S_{\text{ch}}^{\text{in}}Y > \varphi_0$, $S_{\text{ch}}^{\text{in}}Y + S_{\text{ph}}^{\text{in}}Y_4 > \varphi_0 + \varphi_1$	$c_3 > 0$, $c_5 > 0$, $r_4 > 0$, $r_5 > 0$
SS7	$\mu_1\left(S_{\text{ph}}^{\text{in}}Y_4, S_{\text{H}_2}^{\text{in}}\right) > D + a_1$	$S_{\text{ph}}^{\text{in}}Y_4 + S_{\text{H}_2}^{\text{in}} < M_1\left(D + a_1, M_3\left(S_{\text{ch}}^{\text{in}}Y, D + a_0\right)\right) + M_3\left(S_{\text{ch}}^{\text{in}}Y, D + a_0\right)$, $S_{\text{ph}}^{\text{in}}Y_4 + S_{\text{H}_2}^{\text{in}} < \varphi_1(D) + M_2(D + a_2)$
SS8	$S_{\text{ph}}^{\text{in}}Y_4 > \varphi_1(D)$, $S_{\text{ph}}^{\text{in}}Y_4 + S_{\text{H}_2}^{\text{in}} > \varphi_1(D) + M_2(D + a_2)$	$S_{\text{ch}}^{\text{in}}Y < \varphi_0(D)$

B TABLES

Table 4: Definitions of the surfaces Γ_i, $i = 1, \ldots, 12$ where s_0 is the solution of $\psi_0(s_0) = D + a_0$ and s_2^{*i}, $i = 1, 2$ are the solutions of $\Psi(s_2, D) = (1-\omega)Y S_{\text{ch}}^{\text{in}} + Y_4 S_{\text{ph}}^{\text{in}} + S_{\text{H}_2}^{\text{in}}$.

$\Gamma_1 = \left\{\left(S_{\text{ch}}^{\text{in}}, S_{\text{ph}}^{\text{in}}, S_{\text{H}_2}^{\text{in}}, D\right),\ S_{\text{ch}}^{\text{in}}Y(1-\omega) = \phi_1(D) - S_{\text{ph}}^{\text{in}}Y_4 - S_{\text{H}_2}^{\text{in}}\right\}$
$\Gamma_2 = \left\{\left(S_{\text{ch}}^{\text{in}}, S_{\text{ph}}^{\text{in}}, S_{\text{H}_2}^{\text{in}}, D\right),\ S_{\text{ch}}^{\text{in}}Y(1-\omega) = \phi_2(D) - S_{\text{ph}}^{\text{in}}Y_4 - S_{\text{H}_2}^{\text{in}}\right\}$
$\Gamma_3 = \left\{\left(S_{\text{ch}}^{\text{in}}, S_{\text{ph}}^{\text{in}}, S_{\text{H}_2}^{\text{in}}, D\right),\ r_5\left(D, S_{\text{ch}}^{\text{in}}, S_{\text{ph}}^{\text{in}}, S_{\text{H}_2}^{\text{in}}\right) = 0\right\}$
$\Gamma_4 = \left\{\left(S_{\text{ch}}^{\text{in}}, S_{\text{ph}}^{\text{in}}, S_{\text{H}_2}^{\text{in}}, D\right),\ S_{\text{ch}}^{\text{in}}Y = M_0\left(D + a_0, S_{\text{H}_2}^{\text{in}}\right)\right\}$
$\Gamma_5 = \left\{\left(S_{\text{ch}}^{\text{in}}, S_{\text{ph}}^{\text{in}}, S_{\text{H}_2}^{\text{in}}, D\right),\ S_{\text{ch}}^{\text{in}}Y = \varphi_0(D)\right\}$
$\Gamma_6 = \left\{\left(S_{\text{ch}}^{\text{in}}, S_{\text{ph}}^{\text{in}}, S_{\text{H}_2}^{\text{in}}, D\right),\ S_{\text{ch}}^{\text{in}}Y\omega = \text{S}_{\text{H}_2}^{\text{in}} + \omega\varphi_0(\text{D}) - \text{M}_2(\text{D} + \text{a}_2)\right\}$
$\Gamma_7 = \left\{\left(S_{\text{ch}}^{\text{in}}, S_{\text{ph}}^{\text{in}}, S_{\text{H}_2}^{\text{in}}, D\right),\ S_{\text{ch}}^{\text{in}}Y = \varphi_0(D) + \varphi_1(D) - S_{\text{ph}}^{\text{in}}Y_4\right\}$
$\Gamma_8 = \left\{\left(S_{\text{ch}}^{\text{in}}, S_{\text{ph}}^{\text{in}}, S_{\text{H}_2}^{\text{in}}, D\right),\ \mu_1\left(S_{\text{ph}}^{\text{in}}Y_4 + S_{\text{ch}}^{\text{in}}Y - s_0, S_{\text{H}_2}^{\text{in}} - \omega\left(S_{\text{ch}}^{\text{in}}Y - s_0\right)\right) = D + a_1\right\}$
$\Gamma_9 = \left\{\left(S_{\text{ch}}^{\text{in}}, S_{\text{ph}}^{\text{in}}, S_{\text{H}_2}^{\text{in}}, D\right),\ S_{\text{ch}}^{\text{in}}Y = M_0\left(D + a_0, s_2^{*1}\right) + M_1\left(D + a_1, s_2^{*1}\right) - S_{\text{ph}}^{\text{in}}Y_4\right\}$
$\Gamma_{10} = \left\{\left(S_{\text{ch}}^{\text{in}}, S_{\text{ph}}^{\text{in}}, S_{\text{H}_2}^{\text{in}}, D\right),\ S_{\text{ch}}^{\text{in}}Y = M_0\left(D + a_0, s_2^{*2}\right) + M_1\left(D + a_1, s_2^{*2}\right) - S_{\text{ph}}^{\text{in}}Y_4\right\}$
$\Gamma_{11} = \left\{\left(S_{\text{ch}}^{\text{in}}, S_{\text{ph}}^{\text{in}}, S_{\text{H}_2}^{\text{in}}, D\right),\ S_{\text{ph}}^{\text{in}}Y_4 = \varphi_1(D)\right\}$
$\Gamma_{12} = \left\{\left(S_{\text{ch}}^{\text{in}}, S_{\text{ph}}^{\text{in}}, S_{\text{H}_2}^{\text{in}}, D\right),\ D + a_2 = \mu_2\left(S_{\text{H}_2}^{\text{in}}\right)\right\}$

Table 5: Parameter values of the biological parameter $K_{S,H_2,c}$ for cases (1), (2), (3) and (4).

Cases	(A)	(B)	(C)	(D)
$K_{S,H_2,c}$	10^{-6}	4×10^{-6}	6×10^{-6}	7×10^{-6}

C ACKNOWLEDGEMENTS

This work was supported by the UNESCO ICIREWARD project ANUMAB and the Euro-Mediterranean research network TREASURE (http://www.inrae.fr/treasure).

REFERENCES

[1] D. J. Batstone, J. Keller, I. Angelidaki, S.V. Kalyhuzhnyi, S.G. Pavlosthathis, A. Rozzi, W.T.M Sanders, H. Siegrist and V.A. Vavilin, The IWA Anaerobic Digestion Model No 1 (ADM1), *Water Sci Technol*, 45: pages 66–73, 2002.

[2] O. Bernard, Z. Hadj-Sadok, D. Dochain, A. Genovesi and J-P. Steyer, Dynamical model development and parameter identification for an anaerobic wastewater treatment process, *Biotechnol. Bioeng*, 75: pages 424–438, 2001.

[3] M. El-Hajji, N. Chorfi and M. Jleli, Mathematical modelling and analysis for a three-tiered microbial food web in a chemostat, *Electron. J. Diff. Equa*, 255, 2017.

[4] R. Fekih-Salem, Y. Daoud, N. Abdellatif and T. Sari, A mathematical model of anaerobic digestion with syntrophic relationship, substrate inhibition and distinct removal rates, *To appear in SIAM J. Appl. Dyn. Syst. SIADS*, 2021.

[5] S. Nouaoura, N. Abdellatif, R. Fekih-Salem and T. Sari Mathematical analysis of a three-tiered model of anaerobic digestion. *SIAM - Journal on Applied Mathematics (SIAP)*, 81:3, pages 1264–1286, 2021.

[6] S. Nouaoura, R. Fekih-Salem, N. Abdellatif and T. Sari, Mathematical analysis of a three-tiered food-web in the chemostat, *Discrete & Contin. Dyn. Syst. Ser. B*, 26:10, pages 5601–5625, 2021.

[7] S. Nouaoura, R. Fekih-Salem, N. Abdellatif and T. Sari, Operating diagrams for a three-tiered microbial food web in the chemostat, *Preprint, hal-03284354*, 2021.

[8] T. Sari and M. J. Wade, Generalised approach to modelling a three-tiered microbial food-web, *Math. Biosci. J*, 291: pages 21–37, 2017.

[9] S. Sobieszek, M. J. Wade and G. S. K. Wolkowicz, Rich dynamics of a three-tiered anaerobic food-web in a chemostat with multiple substrate inflow, *Math. Biosci. Eng. J*, 17: pages 7045–7073, 2020.

[10] M. J. Wade, R. W. Pattinson, N. G. Parker and J. Dolfing, Emergent behaviour in a chlorophenol-mineralising three-tiered microbial "food web", *Theor. Biol. J*, 389: pages 171–186, 2016.

[11] A. Xu, J. Dolfing, T. P. Curtis, G. Montague and E. Martin, Maintenance affects the stability of a two-tiered microbial "food chain"?, *Theor. Biol. J*, 276: pages 35–41, 2011.